11

Novel Synthetic Route for Tungsten Oxide Nanobundles with Controllable Morphologies

Yun-Tsung Hsieh[1], Li-Wei Chang[1], Chen-Chuan Chang[1],
Bor-Jou Wei[2], and Han C. Shih[1,3*]
[1]*Department of Materials Science and Engineering,*
National Tsing Hua University, Hsinchu, Taiwan,
[2]*Department of Materials Science and Engineering,*
National Chung Hsing University, Taichung, Taiwan,
[3]*Department of Chemical and Materials Engineering,*
Chinese Culture University, Taipei, Taiwan,
R.O.C.

1. Introduction

The formation and characterization of one-dimensional nanomaterials have attracted considerable attention because of their unique physical and chemical properties [1–6]. For example, they can be applied in organic light-emitting diodes (OLEDs), solid lubricants, DNA analysis, and electrochromic devices [7–10]. Because of their semiconducting properties and high surface areas, transition metal oxide nanostructures have been used in a variety of research projects that developed device-oriented nanostructures. For example, tungsten oxide nanostructures such as nanowires, nanorods, nanotubes, nanobelts, and nanofibers have well-known electrical, mechanical, gasochromic, and photoelectrochromic properties that make them very useful for various applications, including field-emission devices, electrochromic devices, light-emitting diodes, and gas and chemical sensors [11–15]. Recently, nanostructured tungsten oxide materials have been of great scientific and applied interest.

Bulk properties such as piezoelectricity, chemical sensing, and photoconductivity of these materials are enhanced in their quasi one-dimensional (Q1D) form. Interestingly, Q1D structures can be used as template for the growth of other nanostructures resulting in novel hierarchical nanoheterostructures with enhanced functionality. Nanosized tungsten oxide particles have been found useful in fabricating gas sensors for the detection of nitrogen oxides, ammonia, and hydrogen sulfide. Current research, however, has focused on the use of polycrystalline tungsten oxide systems for these applications, and thus important sensor requirements such as high sensitivity and reproducibility, which can be obtained only by using size-controlled pure nanomaterials, have not been accomplished.

Cao et al. [16] synthesized WO_3 nanowire by thermal evaporation method, and reported gas sensing tests revealed that the sensor based on the WO_3 nanowire array had the capability of detecting NO_2 concentrations as low as 50 ppb, demonstrating a promising application in

the field of low concentration gas detection. Kim [17] has investigated the dependence of gas-sensing characteristics on thermal treatment conditions in a tungsten oxide nanorod system that demonstrated the facile detection of various analysts at ambient temperature. Thermal treatments under the O_2-containing active environments were found to result in bad reproducibility in sensor response compared with the inert N_2 conditions. As a result, the recommendable thermal treatment conditions for $WO_{2.72}$ sensors were an annealing temperature of 300–500 ◦C under inert N_2 or Ar ambience. The annealing temperature within the range could be utilized as a parameter to regulate a relative population ratio between W^{5+} and W^{6+} states without any noticeable change in morphology or crystalline structure. Sen et al [18] reported that nanowire hierarchical hetero-structures of SnO_2:$WO_{2.72}$ have been prepared by thermal evaporation technique. The density of $WO_{2.72}$ nanowires was found to depend on partial pressure of oxygen and source temperature. Single wires of heterostructures have been aligned between two electrodes to make gas sensors that show high sensitivity and selective response to chlorine gas at room temperature. Improvement in selectivity is attributed to transfer of electrons from $WO_{2.72}$ to SnO_2 on formation of heterojunctions. The study shows the potential of semiconductor oxide hetero-junctions for application to sensors and other electronic devices.

Field emission (FE) (also known as electron field emission) is an emission of electrons induced by external electromagnetic fields. Field emission can happen from solid and liquid surfaces, or individual atoms into vacuum or open air, or result in promotion of electrons from the valence to conduction band of semiconductors. Field emission involves the extraction of electrons from a solid by tunneling through the surface potential barrier. The emitted current depends directly on the local electric field at the emitting surface, E, and on its work function, ϕ, as shown below. In fact, a simple model (the Fowler-Nordheim model, can be written as $J = (E^2\beta^2 / \phi) \exp(-B\ \phi^{1.5} / E\beta)$, where J is the current density, E is the applied electric field, ϕ is the work function (eV), and β is the field enhancement factor) shows that the dependence of the emitted current on the local electric field and the work function is exponential-like. As a consequence, a small variation of the shape or surrounding of the emitter (geometric field enhancement) and/or the chemical state of the surface has a strong impact on the emitted current [19,20].

Tungsten oxide nanowires are one-dimensional nanostructures, with diameters of 10–100 nm and a length of about 1 μm. Since the nanowires have high aspect ratios and are easily fabricated, they have attracted considerable attention as promising materials for field emitters of the field-emission displays (FEDs) [21-23]. Furubayashi et al. [24] have demonstrated that the tungsten oxide nanowires obtained from sputtered tungsten films have good field emission properties. The number density of nanowires was discovered to be an important parameter in determining the field emission properties. A suitably low density resulted in good field emission properties owing to the concentration of the electric field. Concentrating an electric field at the tip of tungsten oxide nanowires increases their emission current. Moreover, they synthesized tungsten oxide nanowires on 1x1 μm^2 islands with various pitches. The lengths of tungsten oxide nanowires were 600–1000 nm and the number of nanowires per island was about 100. It found that the sample with the island pitch of 5μm exhibited the highest field emission current among the samples with pitches of 2, 5, 10, 20 and 30μm.

Among the tungsten oxides, tungsten oxide (WO_3), which is a versatile semiconductor material with a wide bandgap ranging from 2.5–3.6 eV, has strong potential for many interesting applications [25–28]. Methods of synthesizing WO_3 with various morphologies and phases using either physical or chemical routes have been the subject of considerable research. Xu et al. recently synthesized tungsten oxide nanowires using a flame with an air jet impinging on an opposing jet of nitrogen-diluted methane at atmospheric pressure [29]. Klinke et al. found that tungsten oxide nanowires could be formed in a gas mixture of argon, hydrogen, and methane [30]. Wilson et al. reported on a synthesis method that uses tungsten probes 1 m in diameter inserted into an opposed flow of methane oxy-flame with ethane [31].

However, these techniques for making tungsten oxide nanomaterials on substrates require external catalysts or reactants, as well as complicated sample pretreatment and preparation conditions. Furthermore, the importance of substrate temperature in the synthesis of WO_3 nanomaterials has not been considered in previous work. For practical purposes, it is also desirable to develop a simple method for fabricating WO_3 nanobundles of different morphologies, in which appropriate morphology control can be achieved by adjusting the growth parameters. Such a method would yield a thorough understanding of the relationship between the morphologies and properties of the obtained nanobundles. Fabrication of tungsten oxide nanobundles of different morphologies under controlled growth conditions has always been a challenge. As a result, efficient, large-scale fabrication of morphology-controllable tungsten oxide nanobundles is a difficult task.

The thermal chemical vapor deposition (CVD) process offers significant advantages: simple experimental equipment, high homogeneity, very short processing time, cost effectiveness, high efficiency, easy synthesis, and controllability. High quality can be easily obtained with good reproducibility by controlling the CVD parameters [32–34]. Therefore, in the present work, we explore a simple, more economical thermal CVD method for large-scale fabrication of WO_3 nanobundles with controllable morphologies on silicon (100) substrates with no additional catalysts. By heating tungsten powder to 1100°C in vacuum (6.13 Pa) in a two-step process, WO_3 nanobundles with controllable morphologies were produced in high yield; nanowires, nanobars, and nanobulk were produced in furnace temperature ranges of 250–350°C, 450–550°C, and 650–750°C, respectively. Furthermore, in a series of experiments, we successfully achieved room-temperature blue emission from the as-synthesized WO_3 nanobundles, which can be attributed to the band–band indirect transitions of the WO_3 nanobundles.

2. Experimental

In our experiment, we synthesized tungsten oxide nanobundles using thermal CVD. WO_3 nanobundles were synthesized in a conventional horizontal tube furnace made from quartz. Tungsten powder (0.05 g, Alfa AESAR; particle size, 12 μm; purity, 99.99%) acted as the source material; it was deposited on a ceramic boat and placed in the constant-temperature zone of the furnace. A silicon (100) wafer, which acted as the substrate, was subjected to ultrasonic cleaning in ethanol for 30 min and then placed in different temperature zones ranging from 100°C to 800°C, which is about 5 cm downstream from the source. After the tube was pumped to the required vacuum of 0.67–0.8 Pa , the temperature of the furnace was raised from room temperature to 800°C at a ramping rate of 30°C/min. The flow rates

of a mixture of argon and oxygen gases were maintained at 10 sccm and 1 sccm, respectively, and were controlled by a flow meter. The pressure was maintained at 6.13 Pa, and then the temperature of the furnace was increased from 800°C to 1100°C. After this temperature was maintained for 1.2 h, the furnace was cooled naturally to room temperature. Samples formed at substrate temperatures of 250–350°C, 450–550°C, and 650–750°C were removed for characterization.

The deposited nanobundles were then characterized and analyzed. A scanning electron microscope (SEM; JEOL JSM-6500F) was used for morphological analysis. X-ray analysis was performed using a Shimadzu Lab XRD-6000 diffractometer equipped with a graphite monochromator. The Cu Kα radiation had a wavelength of $\lambda = 0.154056$ nm; it was operated at 43 kV and 30 mA. Transmission electron microscopy (TEM) and energy-dispersive x-ray spectroscopy (EDS) were conducted using a JEOL 2010 transmission electron microscope operated at 200 kV. Raman spectroscopy was performed using a micro-Raman setup (LabRAM; Dilor) equipped with a He–Ne laser emitting radiation at 632.8 nm.

The optical properties of the as-prepared nanobundles were measured by cathodoluminescence (CL) spectrometry on a JEOL-JSM-7001F field-emission scanning electron microscope (FESEM) at room temperature. A 15-keV electron beam was used to excite the sample. The CL light was dispersed by a 1200-nm grating spectrometer and detected by a liquid-nitrogen-cooled charge-coupled device.

3. Results

Figure 1 shows SEM images of numerous high-density tungsten oxide nanobundles formed at different substrate temperatures. The morphology of the WO_3 nanobundles on the silicon substrate clearly reveals the formation of nanowires, nanorods, and nanobulk material. The SEM image in Fig. 1a clearly demonstrates that the nanowires obtained on the substrate at 250–350°C have uniform one-dimensional morphologies and are produced at high density and large scale. The nanowires had diameters of 20–30 nm and lengths of up to several nanometers. The as-synthesized nanowires have a high aspect ratio similar to that reported previously [35]. Figure 1b shows nanorods prepared on the substrate at 450–550°C. The average lengths of these nanorods were 400–500 nm, and their diameters were 100–150 nm, and they have polygonal cross sections. It is apparent that the nanorods are formed by an increase in the diameter of the nanowires. Figure 1c shows nanobulk material that covered the entire surface of the substrate at 650–750°C. The material consists of polyhedrons with an average diameter of up to 300 nm and lengths of up to hundreds of nanometers.

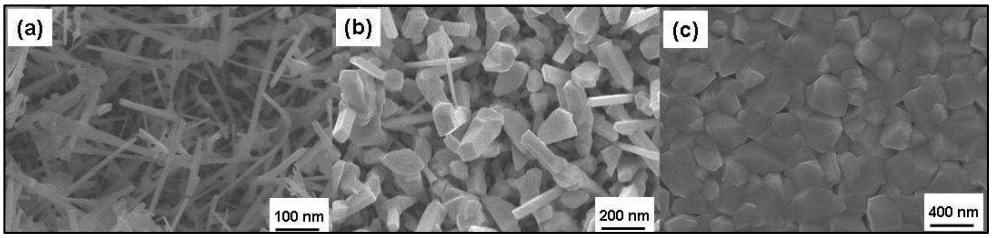

Fig. 1. SEM images of tungsten oxide nanobundles formed at different substrate temperatures: (a) 250–350°C, (b) 450–550°C, (c) 650–750°C.

The phases of the as-prepared WO_3 nanobundles were identified by XRD. Figure 2 shows XRD spectra of WO_3 nanobundles fabricated at three different substrate temperatures. All the spectral peaks were indexed well to monoclinic WO_3 in accordance with the Joint Committee on Powder Diffraction Standards (JCPDS) card No. 43-1035 (lattice constants: a = 0.7297 nm; b = 0.7539 nm; c = 0.7688 nm; β = 90.91°). No diffraction peaks corresponding to tungsten oxides other than WO_3 could be detected in the spectra. Strong, sharp diffraction peaks also indicate good crystallinity in the as-synthesized product. The (002) diffraction peak shows the strongest diffraction, indicating that [002] is the major growth direction of the nanobundles. Moreover, the intensity of the (002) peak was found to increase with increasing substrate temperature. This may reflect the increasing volume of the nanobundles with increasing substrate temperature. However, the distribution and alignment of the nanobundles whose spectra appear in Fig. 2 may vary with substrate temperature. This change in distribution and alignment may also change the relative intensities of the (002), (200), (120), and (140) peaks in the XRD spectra. Further, the intensities of the (022), (202), and (114) diffraction peaks also increased with increasing substrate temperature. This behavior indicates that the [002] growth direction also influence all three peaks with increasing substrate temperature.

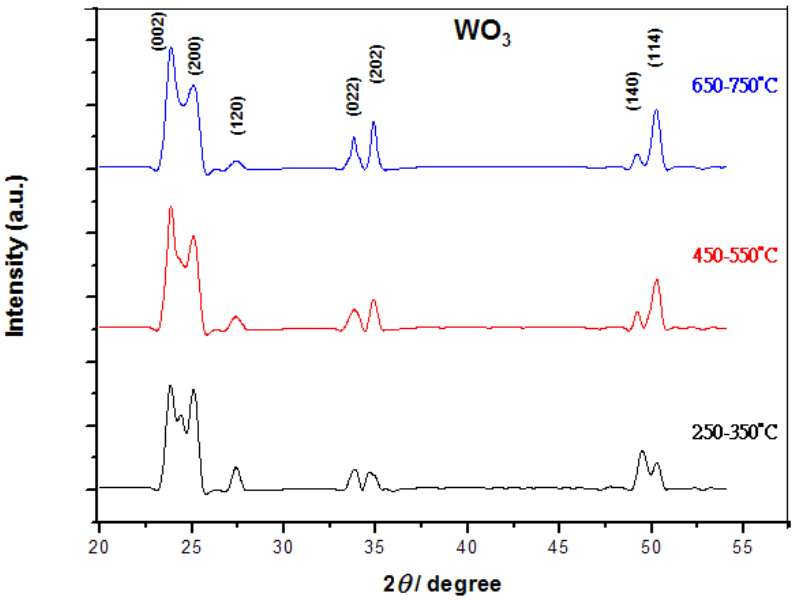

Fig. 2. XRD spectra of the nanobundles fabricated at substrate temperatures of 250–350°C, 450–550°C, and 650–750°C.

We further studied the morphologies of the as-prepared nanobundles by TEM. Figure 3a shows a typical low-magnification TEM image of a straight nanowire with a uniform diameter (25 nm). The crystal structure and growth direction of individual nanowires are further investigated by high-resolution TEM (HRTEM), as shown in Fig. 3b. The inset in this figure shows the selected-area diffraction (SAD) pattern along the [100] zone axis. It reveals that the nanowire has a single-crystal structure. The lattice spacings are 0.385 and 0.379 nm

along the two orthogonal directions, which correspond to the (002) and (020) planes of monoclinic WO_3, respectively. The SAD pattern shown in the inset of Fig. 3b also confirms that the nanowires exhibit the monoclinic WO_3 phase (JCPDS 43-1035). Figure 3c shows a typical low-magnification TEM image of the obtained nanorods (width: 120 nm). The HRTEM image shown in Fig. 3d shows the crystal structure and growth direction of the individual nanorod in Fig. 3c. The measured lattice spacings along the two orthonormal directions are 0.385 and 0.379 nm, which correspond to the (002) and (020) planes of monoclinic WO_3, respectively. The measured lattice spacing and SAD pattern show that the nanobundles are single crystalline and that the major growth direction is [002].

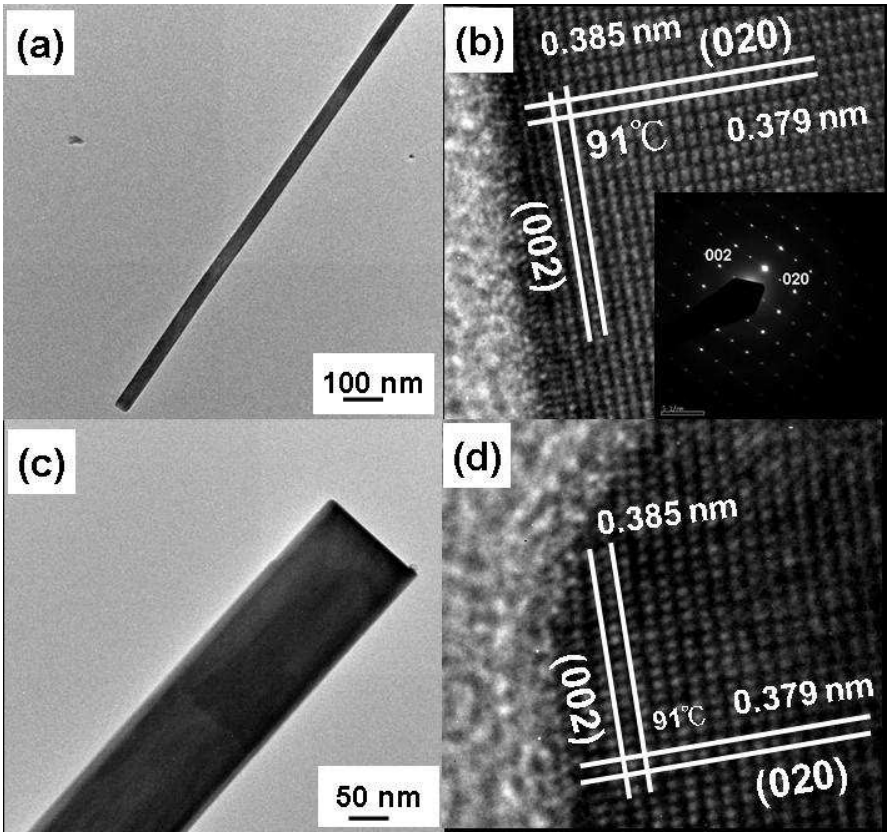

Fig. 3. (a) TEM and (b) high-resolution TEM (HRTEM) images of a nanowire. Inset shows the corresponding selected-area diffraction (SAD) pattern. (c) TEM and (b) HRTEM images of a nanorod.

Figure 4a shows the corresponding elemental line-scan mapping of the nanowires, revealing that they contain only O and W atoms. Typical EDS data recorded for a single nanowire and a single nanorod (Fig. 4b and 4c) confirm that both these nanobundles are made of WO3 and that the C and Cu signals can be attributed to the Cu grids used for our TEM measurements. Therefore, the WO3 nanobundles fabricated in this study are confirmed to have high purity.

An analysis of individual nanobundles shows that the calculated atomic ratio of W to O is approximately 1:3, which is consistent with the XRD and TEM results obtained for WO3.

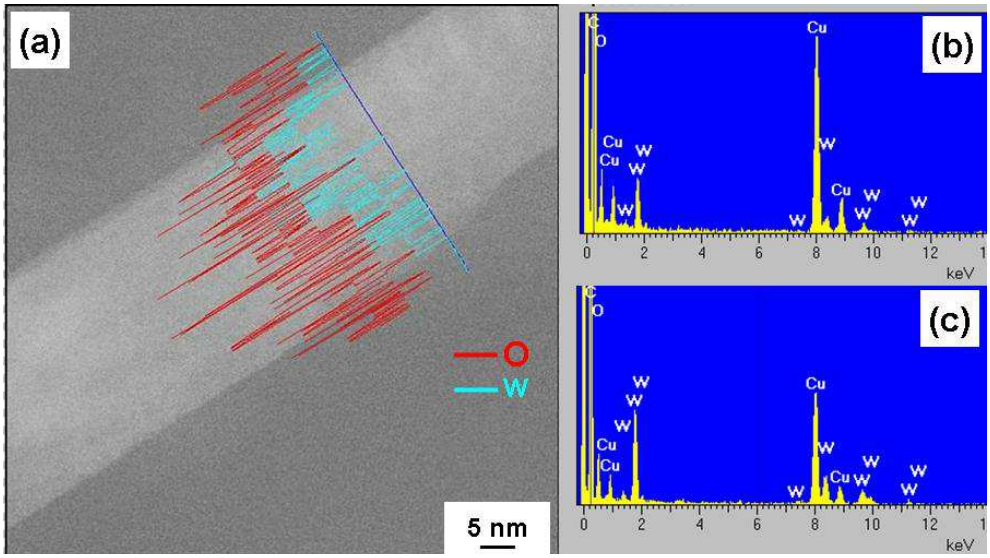

Fig. 4. (a) Energy-dispersive X-ray spectroscopy (EDS) elemental line profile of nanowire shown in Fig. 3a. (b) and (c) EDS spectra for nanobundles fabricated at substrate temperatures of 250–350°C and 450–550°C, respectively. Nanobundles contain only W and O atoms. Peaks due to C and Cu signals can be attributed to copper TEM grids.

To examine the necessary conditions for the growth of WO_3 nanobundles in more detail, we prepared samples using the same method but forming samples on the silicon substrate at different temperatures. Figure 5a, 5b, and 5c shows SEM images of samples synthesized using the same methods and conditions as those for growing the samples shown in Fig. 1; however, the substrate temperatures were 150–250°C, 350–450°C, and 550–650°C, respectively. In Fig. 5a, where the substrate temperature was 150–250°C, almost no nanowires are visible, but many unknown WO_x nanoparticles appear on the substrate. This is because nucleation is difficult with such a low surface energy. In Fig. 5b, where the substrate temperature was 350–450°C, although tungsten oxide nanomaterials were fabricated with high yield, the morphology is disordered. At the substrate temperature of 550–650°C used to fabricate the samples shown in Fig. 5c, the surface energy increased with the substrate temperature and enhanced nucleation. However, the growth environment was still not optimal for producing the required nanobundles but instead yielded unknown tungsten oxide nanomaterials. Thus, these findings unambiguously demonstrate the significant effects of the temperature of the silicon substrate on the WO_3 nanomaterials with controllable morphology.

Finally, the optical properties of the synthesized tungsten oxide nanobundles were characterized by room temperature CL spectroscopy. Figure 6 shows typical CL spectra of the as-prepared WO_3 nanobundles. The strongest CL emission peaks are centered at 351 nm, 350 nm, and 349 nm for substrate temperatures of 250–350°C, 450–550°C, and 650–750°C,

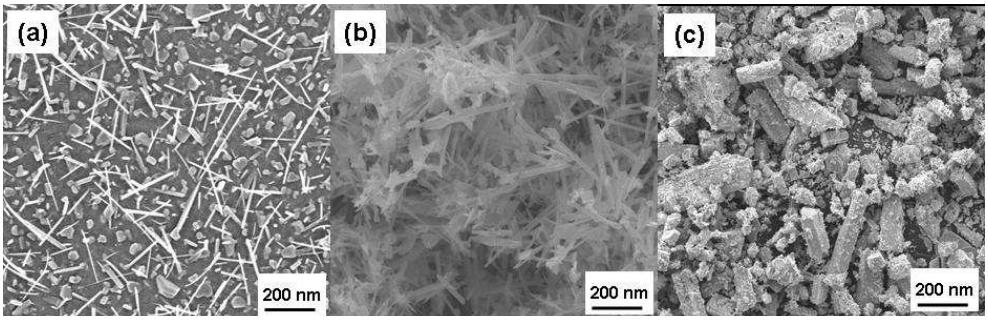

Fig. 5. SEM images of tungsten oxide nanobundles formed at different substrate temperatures: (a) 150–250°C, (b) 350–450°C, (c) 550–650°C.

respectively. Tungsten trioxide is an indirect band gap semiconductor, and its crystals or thin films do not produce such strong luminescence [36]. Single peak at the wavelength has been detected by Lee et al. [37] and Feng et al. [36] They suggested that the peak is due to the intrinsic band–band transition emission induced by quantum confinement effects in nanomaterials with an ultrafine diameter (<5 nm) of individual nanomaterials within each bundle. It is interesting that the nanobundles exhibited a blueshift caused by the increase in diameter with increasing substrate temperature. On the other hand, other origins such as foreign matter or native defects in the structure cannot be ruled out.

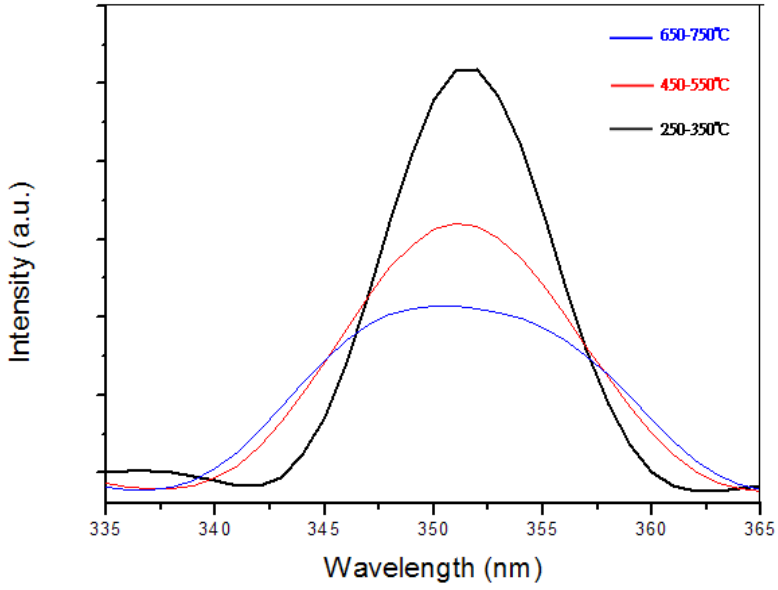

Fig. 6. Cathodoluminescence (CL) spectra of the as-prepared WO_3 nanobundles formed at different substrate temperatures.

4. Discussion

The vapor–solid mechanism is responsible for the growth of WO_3 nanobundles in this experiment, since no catalysts were used [38]. Tungsten powder begins to sublimate from the quartz boat when the temperature is increased to 800°C, and this process is highly enhanced at a temperature of 1100°C. The sublimated tungsten vapor reacts if sufficient oxygen is present. Tungsten trioxide vapor subsequently flows to the lower-temperature zone where the silicon substrate is located and becomes supersaturated, with nucleation of small clusters and subsequent growth of nanobundles. A previous report revealed that when the vacuum is not high enough, the mean free path of the vapor in the furnace is small; this affects the degree of supersaturation over the substrate and thereby obstructs the nucleation process [39]. On the other hand, when the vacuum becomes significantly higher, such that the mean free path of the tungsten trioxide vapor is highly enhanced, its partial pressure, and hence supersaturation, increases in the substrate zone in which the nucleation of WO_3 on the silicon substrate has been enhanced. In this growth process, if the furnace has a vacuum of intermediate strength, nucleation on the silicon substrate is rare. Increasing the temperature and selecting a suitable gas flux and substrate temperature promote nucleation by modifying the adsorption and diffusion characteristics of the surface. This increases the efficiency of nucleation, thereby promoting nanobundle growth. It is extremely interesting to compare our results with those of studies in which WO_3 nanostructures are fabricated on a silicon substrate using different types of catalyst [40, 41].

For reasons of practicality and efficiency, we tried to produce tungsten oxide nanobundles while controlling fewer experimental parameters. We found that different substrate temperatures can produce different nanomaterials, including nanowires, nanorods, and nanobulk, under a suitable growth environment. However, the mechanism responsible for the formation of different tungsten oxide nanobundles is not yet fully understood. Ye et al. [42] reported that the growth rate of the crystals was generally determined by gas-phase supersaturation of the species of the growth material, and that the shape of the final crystal was determined by the surface energy of the planes of the growing surface. These conclusions can also explain the growth process in our study. To our knowledge, the observed types of tungsten oxide nanobundle, i.e., nanowires, nanorods, and nanobulk, may be directly related to the principal factor in our experiment, substrate temperature. During growth, the surface energy increases with increasing substrate temperature, facilitating easy and efficient nucleation. Therefore, the growth of various nanobundles was influenced by changing the substrate temperature.

5. Conclusions

We fabricated WO_3 nanobundles by thermal chemical vapor deposition via a two-step heating process with no catalyst. By simply varying the substrate temperatures, several types of uniform, single-crystalline WO_3 nanobundles can be formed, such as nanowires, nanorods, and nanobulk. This method is simple, effective, catalyst-free, and easily repeatable; further, it affords the desired nanobundles in very large yields. Thus, this method is highly suitable for the fabrication of WO_3 nanobundles. The fabricated

nanobundles can be used in gas and chemical sensors, field-emission devices, electrochromic devices, and light-emitting diodes.

In a future study, we intend to apply this more efficient and controllable fabrication method to the synthesis of metal–semiconductor composite nanoarchitectures with promising structural, morphological, and electrochemical properties.

6. Acknowledgments

This research was supported by the National Science Council through Grant No. 96-2221-E-034-006-MY2 and No.98-2221-E-034-007-MY2.

7. References

[1] P. E. Hovsepian, A. P. Ehiasarian, Y. P. Purandare, R. Braun and I. M. Ross, Plasma Process Polym., 6 (2009) S118

[2] L. Gao, R. L. Woo, B. Liang, M. Pozuelo, S. Prikhodko, M. Jackson, N. Goel, M. K. Hudait, D. L. Huffaker, M. S. Goorsky, S. Kodambaka and R. F. Hicks, Nano Lett., 9 (2009) 2223

[3] M. Stuber, H. Leiste, S. Ulrich, H. Holleck and D. Schild, Surf. Coat. Tech., 150 (2002) 218

[4] K. Fadenberger, I. E. Gunduz, C. Tsotsos, M. Kokonou, S. Gravani, S. Brandstetter, A. Bergamaschi, B. Schmitt, P. H. Mayrhofer, C. C. Doumanidis and C. Rebholz, Appl. Phys. Lett., 97 (2010) 144101

[5] F. Pinakidou, M. Katsikini, P. Patsalas, G. Abadias and E. C. Paloura, J. Nano Res., 6 (2009) 43

[6] M. McNallan, D. Ersoy, R. Zhu, A. Lee, C. White, S. Welz, Y. Gogotsi, A. Erdemir and A. Kovalchenko, Tsinghua Sci. Technol., 10 (2005) 699

[7] C. J. Chiang, S. Bull, C. Winscom and A. Monkman, Org. Electron., 11 (2010) 450

[8] D. Medaboina, V. Gade, S. K. R. Patil and S. V. Khare, Phys. Rev. B, 76 (2007) 205327

[9] X. Zhang, B. Luster, A. Church, C. Muratore, A. A. Voevodin, P. Kohli, S. Aouadi and S. Talapatra, Appl. Mat. Interfaces, 1 (2009) 735

[10] B. M. Venkatesan, B. Dorvel, S. Yemenicioglu, N. Watkins, I. Petrov and R. Bashir, Adv. Mater., 21 (2009) 2771

[11] X. Li, G. Zhang, F. Cheng, B. Guo and J. Chen, J. Electrochem. Soc., 153 (2006) H133

[12] Y. D. Huh, J. H. Shim, Y. Kim and Y. R. Do, J. Electrochem. Soc., 150 (2003) H57

[13] K. Huang, Q. Pan, F. Yang, S. Ni and D. He, Physica E, 39 (2007) 219

[14] S. Sen, P. Kanitkar, A. Sharma, K. P. Muthe, A. Rath, S. K. Deshpande, M. Kaur, R. C. Aiyer, S. K. Gupta and J. V. Yakhmi, Sensor. Actuat. B-Chem., 147 (2010) 453

[15] R. Seelaboyina, J. Huang, J. Park, D. H. Kang and W. B. Choi, Nanotechnology, 17 (2006), 4840

[16] B. Cao, J. Chen, X. Tang, and W. Zhou, "Growth of monoclinic WO_3 nanowire array for highly sensitive NO_2 detection", *J. Mater. Chem.*, 19, 2323 (2009).

[17] Y. S. Kim, *Sensor.* "Thermal treatment effects on the material and gas-sensing properties of room-temperature tungsten oxide nanorod sensors", *Actuat. B-Chem.*, 137, 297 (2009).
[18] S. Sen, P. Kanitkar, A. Sharma, K. P. Muthe, A. Rath, S. K. Deshpande, M. Kaur, R., "Growth of SnO_2/WO2.72 nanowire hierarchical heterostructure and their application as chemical sensor", *Sensor. Actuat. B-Chem.*, 147, 453 (2010).
[19] K. Huang, Q. Pan, F. Yang, S. Ni, and D. He, "Synthesis and field-emission properties of the tungsten oxide nanowire arrays", *Physica. E*, 39, 219 (2007).
[20] Y. M. Zhao, Y. H. Li, I. Ahmad, D. G. Mccartney, and Y. Q. Zhu, "Two-dimensional tungsten oxide nanowire networks", *Appl. Phys. Lett.*, 89, 133116 (2006).
[21] K. Huang, Q. Pan, F. Yang, S. Ni, and D. He, "The catalyst-free synthesis of large-area tungsten oxide nanowire arrays on ITO substrate and field emission properties", *Mater. Res. Bull.*, 43, 919 (2008).
[22] S. Jeon, H. Kim, and K. Yong, "Deposition of tungsten oxynitride nanowires through simple evaporation and subsequent annealing", *J. Vac. Sci. Technol. B*, 27, 671 (2009).
[23] Y. H. Lee, C. H. Choi, Y. T. Jang, E. K. Kim, and B. K. Ju, "Tungsten nanowires and their field electron emission properties", *Appl. Phys. Lett.*, 81, 745 (2002).
[24] M. Furubayashi, K. Nagato, H. Moritani, T. Hamaguchi, and M. Nakao, "Field emission properties of discretely synthesized tungsten oxide nanowires", *Microelectron. Eng.*, 87, 1594 (2010).
[25] M. Boulova and G. Lucazeau, J. Solid State Chem., 167 (2002) 425
[26] J. H. Ha, P. Muralidharan and D. K. Kim, J. Alloy. Compd., 475 (2009) 446
[27] Y. Wu, Z. Xi, G. Zhang, J. Yu and D. Guo, J. Cryst. Growth, 292 (2006) 143
[28] L. G. Teoh, J. Shieh, W. H. Lai, I. M. Hung and M. H. Hon, J. Alloy. Compd., 396 (2005) 251
[29] F. Xu, S. D. Tse, J. F. Al-Sharab and B. H. Kear, Appl. Phys. Lett., 88 (2006) 243115
[30] C. Klinke, J. B. Hannon, L. Gignac, K. Reuter and P. Avouris, *J. Phys. Chem.*, 109 (2005) 17787
[31] M. M. Wilson, S. A. Saveliev, W. C. Jimenez and G. Salkar, Carbon, 48 (2010) 4510
[32] P. C. Chang, Z. Fan, D. Wang, W. Y. Tseng, W. A. Chiou, J. Hong and J. G. Lu, Chem. Mater., 24 (2004) 5133
[33] Q. G. Fu, H. J. Li, X. H. Shi, K. Z. Li, J. Wei and Z. B. Hu, Mater. Chem. Phys., 100 (2006) 108
[34] J.H. Yen, I.C. Leu, M.T. Wu, C.C. Lin and M.H. Hon, Diam. Relat. Mater, 14 (2005) 841
[35] X. L. Li, J. F. Liu and Y. D. Li, Inorg. Chem., 42 (2003) 921.
[36] M. Feng, A. L. Pan, H. R. Zhang, Z. A. Li, F. Liu, H. W. Liu, D. X. Shi, B. S. Zou and H. J. Gao, Appl. Phys. Lett., 86 (2005) 141901
[37] K. Lee, W. S. Seo, J. T. Park, J. Am. Chem. Soc., 125 (2003) 3408
[38] H. Wang, X. Quan, Y. Zhang and S. Chen, Nanotechnology, 19 (2008) 065704
[39] Z. R. Dai, Z. W. Pan and Z. L. Wang, Adv. Funct. Mater., 13 (2003) 9
[40] K. Hong, M. Xie, R. Hu and H. Wu, Nanotechnology, 19 (2008) 085604

[41] J. Zhou, L. Gong, S. Z. Deng, J. C. She and N. S. Xu, J. Appl. Phys., 87 (2005) 223108
[42] C. Ye, X. Fang, Y. Hao, X. Teng and L. Zhang, J. Phys. Chem. B, 109 (2005) 19758.

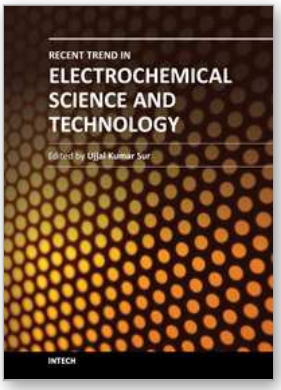

Recent Trend in Electrochemical Science and Technology

Edited by Dr. Ujjal Kumar Sur

ISBN 978-953-307-830-4
Hard cover, 306 pages
Publisher InTech
Published online 27, January, 2012
Published in print edition January, 2012

This book titled "Recent Trend in Electrochemical Science and Technology" contains a selection of chapters focused on advanced methods used in the research area of electrochemical science and technologies; descriptions of electrochemical systems; processing of novel materials and mechanisms relevant for their operation. This book provides an overview on some of the recent development in electrochemical science and technology. Particular emphasis is given both to the theoretical and the experimental aspect of modern electrochemistry. Since it was impossible to cover the rich diversity of electrochemical techniques and applications in a single issue, the focus is on the recent trends and achievements related to electrochemical science and technology.

INTECH
open science | open minds

InTech Europe
University Campus STeP Ri
Slavka Krautzeka 83/A
51000 Rijeka, Croatia
Phone: +385 (51) 770 447
Fax: +385 (51) 686 166
www.intechopen.com

InTech China
Unit 405, Office Block, Hotel Equatorial Shanghai
No.65, Yan An Road (West), Shanghai, 200040, China
中国上海市延安西路65号上海国际贵都大饭店办公楼405单元
Phone: +86-21-62489820
Fax: +86-21-62489821